Planetary and Space Science 63–64 (2012) 150–157

Contents lists available at SciVerse ScienceDirect

Planetary and Space Science

journal homepage: www.elsevier.com/locate/pss

Possible physical cause of the zonal wind collapse on Titan

Jianping Li [a,c,*], Dong Liu [b,c], Athena Coustenis [d], Xinhua Liu [e]

[a] State Key Laboratory of Numerical Modeling for Atmospheric Sciences and Geophysical Fluid Dynamics (LASG), Institute of Atmospheric Physics, Chinese Academy of Sciences, Beijing, China
[b] Research Centre for Strategic Development, China Meteorological Administration, Beijing, China
[c] College of Atmospheric Sciences, Lanzhou University, China
[d] Laboratoire d'Etudes Spatiales et d'Instrumentation en Astrophysique (LESIA), Observatoire de Paris, CNRS, UPMC Université Paris 06, Université Paris-Diderot, 92195 Meudon Cedex, France
[e] National Meteorological Center, China Meteorological Administration, Beijing, China

ARTICLE INFO

Article history:
Received 2 March 2011
Received in revised form
31 August 2011
Accepted 26 September 2011
Available online 12 October 2011

Keywords:
Titan
Zonal wind collapse
Planetary general circulation model (PGCM)
Angular velocity
Superrotation

ABSTRACT

A high-resolution vertical profile of Titan's winds was inferred from ground-based radiotelescopes, which recorded the Doppler Wind Experiment measurements of the carrier frequency during the Huygens mission (Bird et al., 2005). It indicates the existence of a wind shear layer with surprisingly low wind speed nearing zero, at altitudes between 60 and 100 km. We call this phenomenon the 'zonal wind collapse'. Titan's stratosphere is also characterized by an atmospheric superrotation. To identify the physical cause of the zonal wind collapse on Titan, we employ a Planetary General Circulation Model (PGCM) to simulate Titan's general circulation and vertical profiles of the zonal wind under different scenarios of angular velocities. The results show that both the zonal wind collapse and superrotation are closely associated with the magnitude of angular velocity and occur in the slowly rotating regime. This result may be a general phenomenon applicable beyond Titan. In addition, the Community Atmosphere Model version 2 (CAM2) was used to simulate the Earth's atmosphere under different rotation periods for two different physical parameterizations. The zonal wind collapse also observed on Earth is reproduced mainly for a dry atmosphere in the case of rotation periods between 5–50 days and is related to a positive meridional temperature gradient. Besides, a moist process does not only suppress the zonal wind collapse, but also may have an impact on the strength of the superrotation.

1. Introduction

One of Titan's most intriguing attributes is its extended and featureless atmosphere (Coustenis and Taylor, 2008). Some recent studies of Titan's atmosphere have been focusing on circulation (e.g., Hourdin et al., 1995; Grieger et al., 2004; Tokano and Lorenz, 2006), superrotation in the stratosphere (Hourdin et al., 1995; Grieger et al., 2004; Zhu, 2006), hemispheric asymmetry of temperature and haze (e.g., Tokano et al., 1999; Lebonnois et al., 2003; Luz et al., 2003), the feedback of haze distribution on circulation (e.g., Rannou et al., 2004), and other phenomena related to chemical composition (Coustenis et al., 2010 and references within). These studies have improved our understanding of the physical atmospheric processes on Titan. The present study is concerned mainly with the vertical zonal wind and related processes.

Direct measurements from the Doppler Wind Experiment (Bird et al., 2002) on the Huygens probe failed due the loss of the channel A transmission data but were recovered partially, thanks to the monitoring of the channel A signal from the Earth during the Huygens mission by fifteen radio telescopes, six of which recorded ground-based DWE measurements of the carrier frequency (Bird et al., 2005; Lebreton et al., 2005). The recordings have yielded a high-resolution zonal wind height profile of Titan, with an estimated accuracy better than 1 m s^{-1}. The observations indicate that the zonal winds were prograde during most of the Huygens descent through the atmosphere, confirming a superrotation phenomenon (Bird et al., 2005). The wind speed was $\sim$100 m s^{-1} at heights above 120 km. Bird et al. (2005) pointed out that a layer with surprisingly low wind speeds, in which the velocity decreased to near zero (wind shear layer), was detected at altitudes between 60 and 100 km. Very weak winds ($\sim$1 m s^{-1}) could be seen in the lowest 5 km of the atmosphere (see Figure 2 in Bird et al., 2005). The zonal wind speed exceeds 100 m s^{-1} at high altitude, drops rapidly with the decreasing height to near 0 m s^{-1} at heights between 60 and 100 km, and then increases to 40 m s^{-1} at $\sim$50 km. We call this unexpected phenomenon (a sharp decrease of the wind speed

* Corresponding author at: State Key Laboratory of Numerical Modeling for Atmospheric Sciences and Geophysical Fluid Dynamics (LASG), Institute of Atmospheric Physics, Chinese Academy of Sciences, P.O. Box 9804, Beijing 100029, China. Tel.: +86 10 82995181; fax: +86 10 82995172.
E-mail address: ljp@lasg.iap.ac.cn (J. Li).

0032-0633/$ - see front matter © 2011 Elsevier Ltd. All rights reserved.
doi:10.1016/j.pss.2011.09.011

from tens of meters per second at 100 km to a very low wind speed nearing 0 m s^{-1} at heights between 60 and 100 km and then a sharp increase to tens of meters per second) a 'zonal wind collapse', which is just the focus of this study since the possible cause of this zonal wind collapse is not systematically studied before.

General circulation models (GCMs) are an important tool in understanding planetary atmospheric structures, their temporal evolution, and related processes. GCMs have been widely used to successfully simulate the general circulation on Earth. Martian GCMs have been developed by some teams, such as the Geophysical Fluid Dynamics Laboratory (GFDL) (e.g., Wilson and Hamilton, 1996; Wilson et al., 1997); the NASA Ames Research Center (e.g., Pollack et al., 1981, 1990, 1993; Barnes et al., 1993, 1996; Haberle et al., 1993; Murphy et al., 1995; Hollingsworth and Barnes, 1996; Haberle et al., 1999, 2003); Hokkaido University, Japan (Takahashi et al., 2003, 2004); jointly by Oxford University, UK, and Laboratoire de Météorologie Dynamique (LMD) (e.g., Forget et al., 1999; Lewis et al., 1999); the Max Planck Institute for Solar System Research, Germany (e.g., Hartogh et al., 2005, 2007); York University, Canada (e.g., Moudden and McConnell, 2005); and jointly by the Center for Climate System Research of the University of Tokyo and the National Institute for Environmental Studies in Japan (Kuroda et al., 2005). The atmosphere of Venus has also been simulated using GCMs (e.g., Young and Pollack, 1977; Rossow, 1983; Del Genio et al., 1993; Del Genio and Zhou, 1996; Yamamoto and Takahashi, 2003, 2004; Lee et al., 2005, 2007).

GCMs of Titan are developed mainly at Cologne University, Germany (e.g., Tokano et al., 1999; Tokano and Lorenz, 2006) and at the LMD in France (e.g., Hourdin et al., 1995; Lebonnois et al., 2003; Luz et al., 2003; Rannou et al., 2004). A relatively new planetary atmospheric numerical model, Planet WRF (Planetary Weather Research and Forecasting model), has been applied to Mars, Venus, and Titan (Richardson et al., 2007). Dowling et al. (1998) developed an Explicit Planetary Isentropic-Coordinate (EPIC) Atmospheric Model to simulate the atmosphere of the four giant gaseous planets and the middle atmospheres of all planets. This model has also been applied to terrestrial atmospheres (Dowling et al., 2006).

Since 2004 we have developed a transposable planetary general circulation model (PGCM) based on the NCAR's Community Atmosphere Model 2 (CAM2) (Collins et al., 2003) and employed the PGCM to simulate planetary atmospheres, e.g., Titan's atmosphere (Liu et al., 2008). The PGCM is a spectral model that can be adapted to different planetary atmospheres and run in parallel on different operating systems. The PGCM could be used to investigate characteristics and physical processes of various planetary atmospheres. In the previous paper (Liu et al., 2008) the PGCM was used to simulate successfully the circulation in Titan's atmosphere and was validated in different conditions of the satellite's physical processes.

In this study, we employ the PGCM to simulate Titan's atmosphere under different angular velocities/rotation periods (i.e., 1, 5, 10, 16, 50, and 243 Earth days, among which the rotation periods of Titan and Venus are 16 and 243 days, respectively) to identify any dependence of the characteristics of circulation, vertical zonal wind, and other factors, especially the phenomenon of the zonal wind collapse, on different scenarios of angular velocity. In addition, superrotation conditions are also discussed.

The remainder of this paper is organized as follows. The model and experimental design are described in Section 2. Section 3 presents the PGCM experimental results and analysis regarding the zonal wind collapse and superrotation on Titan. Section 4 discusses zonal wind collapse and superrotation on Earth under different scenarios of angular velocities and makes some comparisons with the PGCM simulation on Titan. Section 5 provides a summary of our conclusions.

2. Model description and experimental design

The PGCM is a spectral model based on CAM2 (for details of CAM2, see Collins et al., 2003). CAM2 was modified to enable its application to various planetary atmospheres (Liu et al., 2008). The PGCM differs from CAM2 mainly in terms of the orbital constants, some constants and parameterizations of the physical processes, the number of vertical levels, the vertical coordinates, the time step-size, the adoption of generalized planetary timing, etc. However, the PGCM is the same as CAM2 when it is used to simulate Earth's atmosphere.

In the PGCM, the horizontal representation of an arbitrary variable consists of a truncated series of spherical harmonic functions. It adopts sigma coordinates (as commonly used as a vertical coordinate in general circulation models, where σ is the pressure normalized to its surface value) and is integrated in time using the semi-implicit leapfrog scheme. The relatively flat topography on Titan (Radebaugh et al., 2007) means that the relief does not influence the global surface wind pattern except locally pronounced regions (e.g., at Xanadu and Tsegihi) (Tokano, 2007). Therefore, the topography is not considered in the present analysis and the vertical coordinate is changed from hybrid coordinates to sigma coordinates. In short, the model grids are based on 64 Gaussian latitude points and 128 longitude points (at an interval of 2.8125) in the horizontal plane, and the vertical resolution is 26 layers with σ-levels.

We performed PGCM simulations of the general circulation of Titan under different scenarios of angular velocities/rotation periods (i.e., 1, 5, 10, 16, 50, and 243 days). The results obtained for each angular velocity/rotation period are compared in terms of the zonal wind collapse, atmospheric superrotation, and meridional circulations to identify the effects of angular velocity/rotation period on them. For comparison, we also conducted CAM2 simulations of Earth's atmosphere under different angular velocities/rotation periods (i.e., 0.5, 1, 5, 10, 16, 50, 150, and 243 days). In the CAM2 runs, two physical parameterizations, an idealized parameterization of physical processes and a complete physical parameterization, are used. In the idealized parameterization (Held and Suarez, 1994; Williamson et al., 1998), dry convective adjustments are employed (i.e., moist process is ignored), the only specified dissipation is a simple linear damping of the velocity, which is non-zero only in layers near the surface. Besides, topography is not taken into account.

Fig. 1 shows the time evolution of the global average of the vertical integration of atmospheric kinetic energy per unit mass from PGCM, which represents the model's spin-up phase. The transition of the global angular momentum to equilibrium is shown for all simulations. All the numerical experiments attained equilibrium after about 5 Titan years. After the vertical integration of the atmospheric kinetic energy per unit mass has reached a steady-state regime, the value is minimized (0.4) at the rotation period of the Earth (1 day), increases to a maximum (5.6) at the rotation period of 50 days, and then decreases to about 2.2 at the rotation period of 243 days. This result shows that at the rotation period of 50 days, the atmosphere rotates the fastest in terms of mean angular momentum. To achieve a stable numerical result, therefore we carried out a 6 Titan years run of the PGCM. The results of the sixth Titan year are used to analyze the Titan-like atmospheric climatological circulation.

3. Zonal wind collapse and superrotation on Titan

The zonal wind collapse is a remarkable feature of the vertical profile of the wind on Titan (Bird et al., 2005), as mentioned above, showing that superrotation occurs at heights above 10 mbar in the stratosphere, where the zonal wind speed exceeds

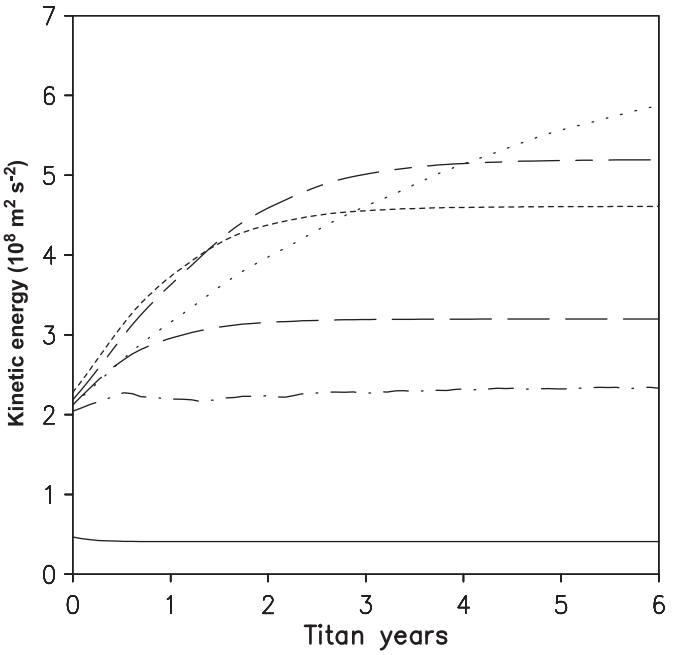

Fig. 1. Time evolution of the global average of the vertical integration of atmospheric kinetic energy per unit mass from PGCM for the rotation periods of 1 day (solid line), 5 days (long-dashed line), 10 days (short-dashed line), 16 days (long–short dashed line), 50 days (dotted line), and 243 days (dot-dashed line). Unit: 10^8 m^2 s^{-2}.

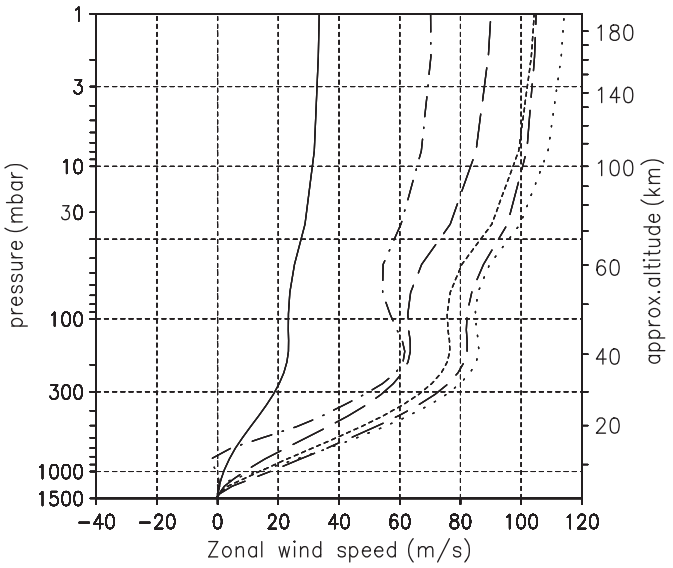

Fig. 2. PGCM simulated vertical profiles of annual zonal-mean zonal wind at 10°S on Titan for the rotation periods of 1 day (solid line), 5 days (long-dashed line), 10 days (short-dashed line), 16 days (long–short dashed line), 50 days (dotted line), and 243 days (dot–dashed line). Unit: m s^{-1}.

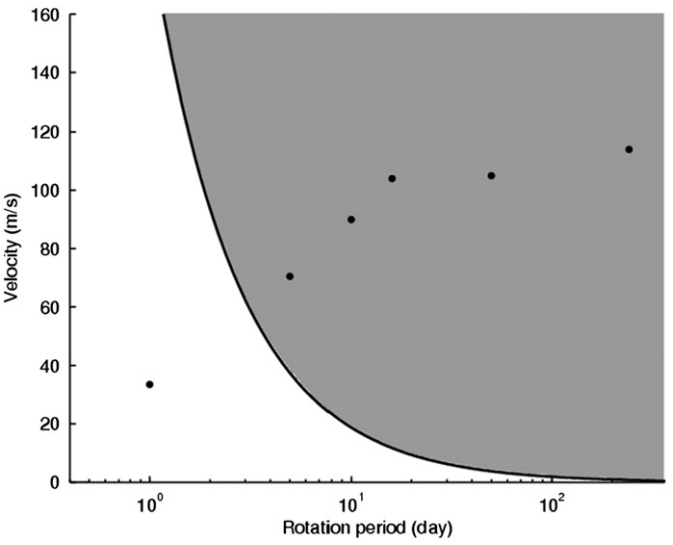

Fig. 3. Linear velocity at the equator (solid curve, m s^{-1}) and superrotation regime (shaded area) for Titan conditions versus rotation period (day). Dots are the PGCM simulated maximum values of annual zonal-mean zonal wind (m s^{-1}) at 10°S on Titan for the rotation periods of 1 day, 5, 10, 16, 50, and 243 days.

100 m s^{-1}. The zonal wind speed shows a sharp decrease with decreasing height in the upper stratosphere, with the minimum ($\sim$3 m s^{-1}) at altitudes between 20 and 30 mbar. It then shows a rapid increase with the decreasing height in the lower stratosphere, attaining a maximum ($\sim$35 m s^{-1}) at altitudes between 40 and 50 mbar. The vertical profile of the zonal wind speed shows a collapse at heights near 20 and 30 mbar. Below 50 km height, the zonal wind velocity decreases with the decreasing height, attaining a minimum (weak easterly wind) near the surface. The rate of wind decrease in this layer is evidently smaller than that in the upper stratosphere.

Fig. 2 shows the PGCM simulated vertical profiles of annual zonal-mean zonal wind at 10°S on Titan, near which latitude the Huygens probe landed, under different scenarios of rotation periods. It can be seen from Fig. 2 that there is no zonal wind collapse at Earth's rotation period of 1 day, and it occurs only when the rotation period exceeds 5 days, however, the intensity is weaker, compared with the observations. Besides, the simulated height of the zonal wind collapse is lower than the real one as well. In general, the zonal winds in the whole atmosphere are westerly. For a rotation period of less than 50 days, the zonal wind speed increases with the increasing rotation period at a given height. For the rotation period of 243 days, the zonal wind speed is slower than that at 5 days but faster than that at the Earth's rotation period. The zonal winds are very weak near the surface. In particular, at the rotation period of 243 days a weak easterly wind develops below 850 mbar. Below 200 mbar in all the experiments, the zonal wind velocity increases with the increasing height. The velocity reaches a maximum at $\sim$200 mbar, with the largest value being $\sim$85 m s^{-1} for the rotation period of 50 days. At altitudes between 30 and 200 mbar, there exists a weak collapse in the vertical zonal wind profiles, where the zonal wind velocity decreases with the increasing altitude from the lower layer and then increases after attaining a minimum. This result implies that a zonal wind collapse happens in the circumstances of a larger rotation period or a slower angular velocity.

The minimum values of zonal wind and corresponding heights between 30 and 200 mbar are dependent on the rotation period. At above 30 mbar for all the experiments, the zonal wind velocity increases with the increasing height (Fig. 2). A pronounced feature of the simulated zonal wind profiles is that the superrotation happens under the circumstance of the slowly rotating regime (Fig. 3). Similar to Del Genio et al. (1993) and Del Genio and Zhou (1996), we find the strength of superrotating zonal winds to increase with rotation period in the slowly rotating regime. However, the growth rate of the strength is very small for the larger rotation periods. For instance, all the maximum values for the rotation periods of 16, 50, and 243 days are around 110 m s^{-1}. We may use a semi-geostrophic balance theory to explain the superrotation that might be an intrinsic feature of atmosphere on slowly rotating planets with stable radiative

equilibrium structures. For large-scale motion and long-term average of atmosphere we may have a semi-geostrophic balance below (for Earth's atmosphere, see Li and Chou, 1998; Holton, 2004) if the advection and frictional force could be neglected,

$$u \approx -\frac{1}{\rho f}\frac{\partial p}{\partial y},$$

where u is the zonal wind, ρ the air density, p the pressure, and f the Coriolis parameter. For a planet with a dry atmosphere and a stable radiative equilibrium structure, the thermal state of the atmosphere is stable, and thus the zonal wind is inversely proportional to the Coriolis parameter, i.e., the slower the rotating, the stronger the zonal wind.

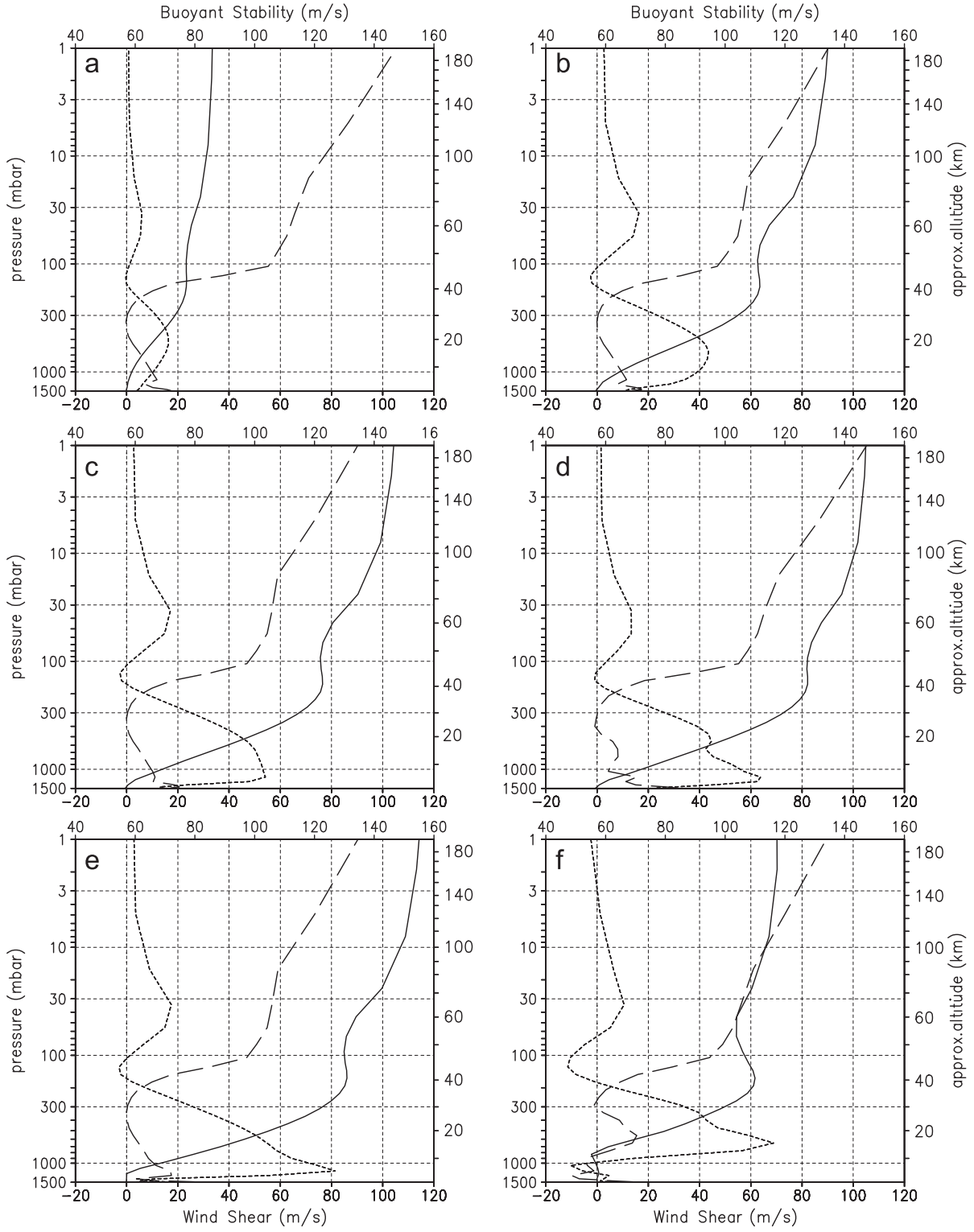

Fig. 4. PGCM simulated vertical profiles of zonal-mean zonal wind (solid lines), wind shear per scale-height (short-dashed line), and buoyant stability (long-dashed line) at 10°S on Titan, for rotation periods of 1 day (a), 5 days (b), 10 days (c), 16 days (d), 50 days (e), and 243 days (f). Unit: m s^{-1}.

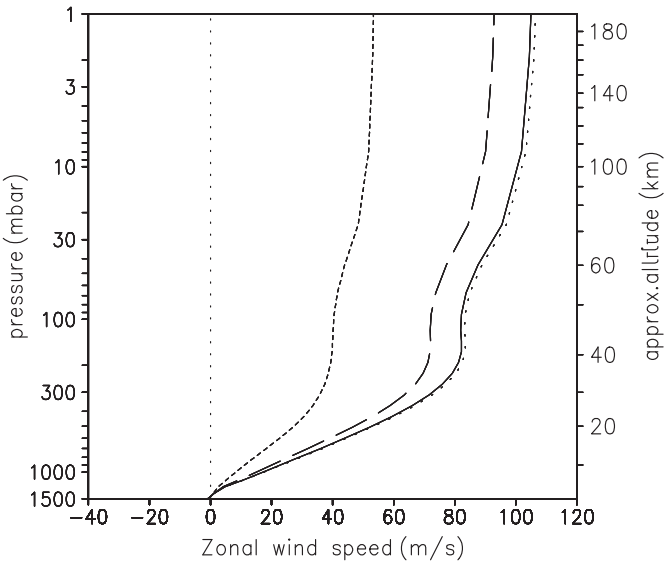

Fig. 5. Same as for Fig. 2, but only for the rotation period of 16 days and for latitudes of 0° (dotted line), 10°S (solid line), 30°S (long-dashed line), and 60°S (short-dashed line). Unit: m s^{-1}.

Fulchignoni (2007) calculated buoyant stability above the equator and found that it first increases and then decreases with the decreasing height at the altitude where the zonal wind collapse occurs. Here we calculate both buoyant stability and zonal wind shear in an effort to identify a possible physical linkage between the zonal wind collapse and buoyant stability. The wind shear and buoyant stability are given by $\partial u/\partial\hat{z}$ and NH, respectively, where $\hat{z}=\ln(p_0/p)$, p_0=1500 mbar, the Bruat frequency is $N=\frac{g}{RT}[R(\partial T/\partial\hat{z}+RT/c_p)]^{1/2}$, the scale height $H=RT/g$, R the gas constant for dry air, T the air temperature, g the acceleration due to gravity, and c_p the specific heat capacity of dry air at constant pressure. Fig. 4 shows the vertical profiles of the zonal-mean zonal wind, wind shear per scale-height, and buoyant stability at 10°S on Titan from PGCM. A remarkable feature from Fig. 4 is that negative wind shear occurs in the layer between 100 and 200 mbar in the slowly rotating regime and above the layer (around 30–40 mbar) there is a maximum value of wind shear, corresponding to the zonal wind collapse. Above 30 mbar, the wind shear decreases with the increasing height, approaching zero in the upper stratosphere. It can be seen from Fig. 4 that there are three obvious turning points in the vertical profiles of buoyant stability (at approximately 20, 100, and 200 mbar), coinciding with turning points for the zonal wind speed. The slope of buoyant stability between 100 and 200 mbar is the lowest and between 20 and 100 mbar is the largest, which might be related with the zonal wind collapse.

The zonal wind collapse varies with latitude. Fig. 5 shows the simulated vertical profiles of annual zonal-mean zonal wind at different latitudes (the equator, 10°S, 30°S, and 60°S) on Titan. It can be seen that the zonal winds are mainly westerly at all latitudes, with the wind speed increasing with increasing latitude for a given height, and the zonal wind speed at a given altitude decreasing with increasing latitude. The superrotation happens not only in the lower latitudes but also at high latitudes. Differently from the superrotation, however, the zonal wind collapse is not apparent at high latitudes.

4. Zonal wind collapse and superrotation on Earth under different scenarios of angular velocities

To further understand the zonal wind collapse and superrotation and make a comparison with the Titan simulations, we conducted

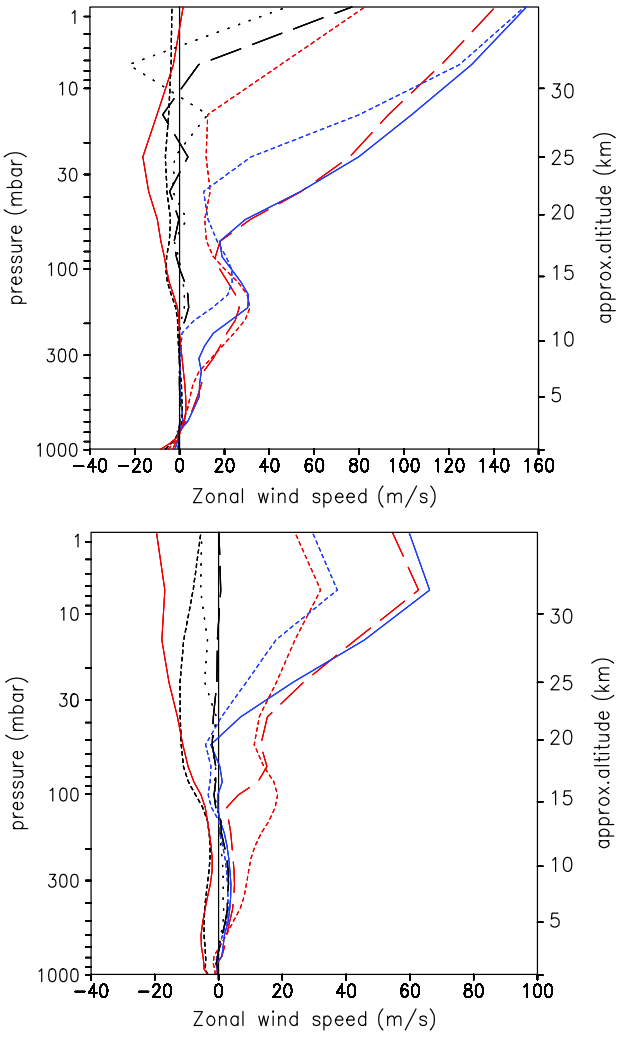

Fig. 6. Same as in Fig. 2, but for the CAM2 runs with an idealized physical parameterization (upper) and complete physical parameterization (lower) for the rotation periods of 0.5 day (short-dashed line), 1 day (red solid line), 5 days (red short-dashed line), 10 days (red long-dashed line), 16 days (blue solid line), 50 days (blue short-dashed line), 150 days (long-dashed line), and 243 days (dotted line). Unit: m s^{-1}.

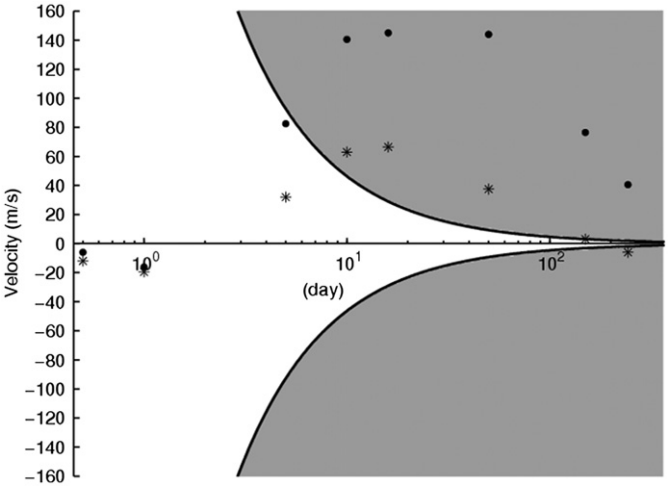

Fig. 7. Same as in Fig. 3 but for Earth condition. Dots and stars are the CAM2 simulation of the idealized physical parameterization and complete physical parameterization for the rotation periods of 0.5 day, 1 day, 5, 10, 16, 50, and 243 days, respectively.

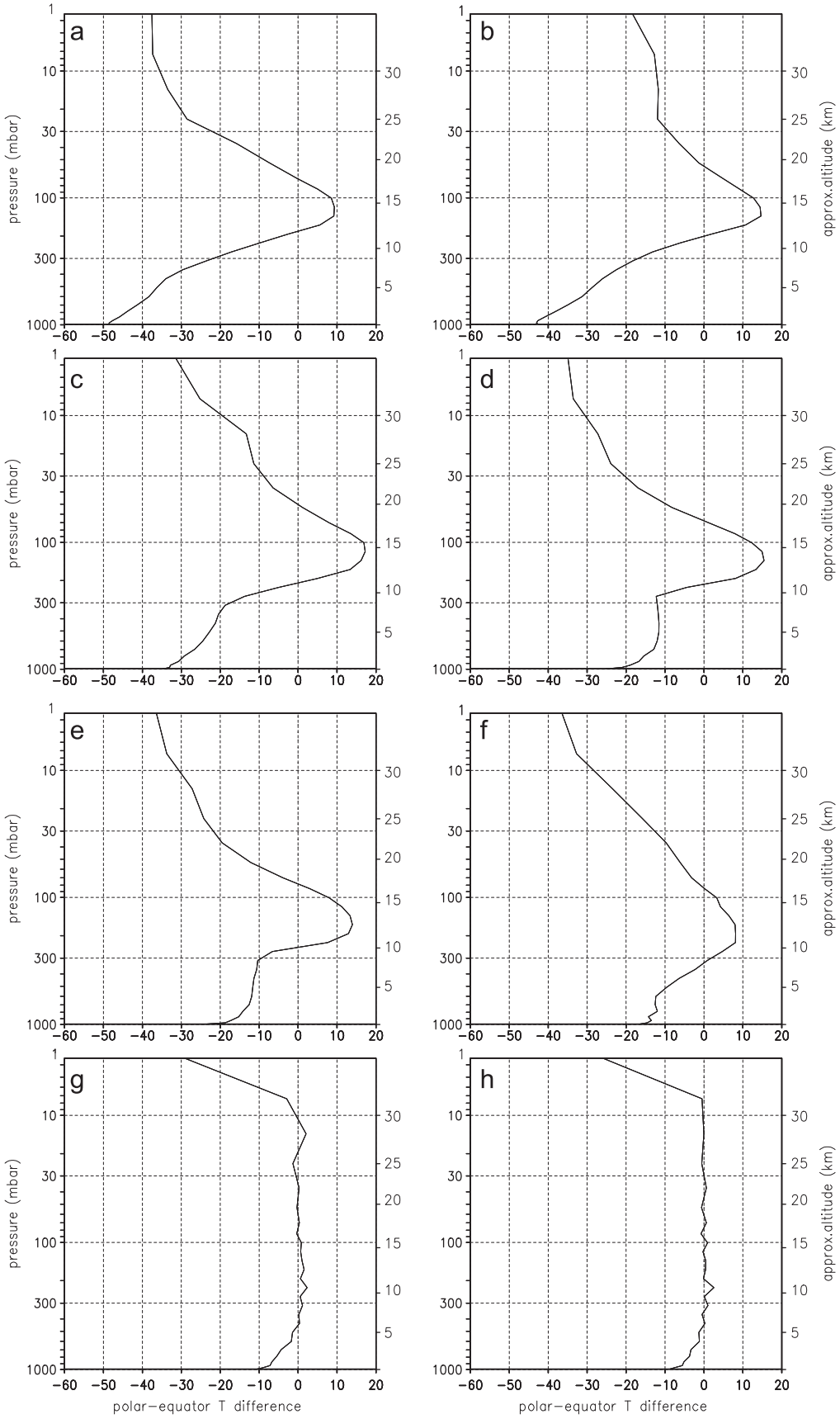

Fig. 8. Vertical profiles of annual polar–equator temperature difference (solid line) from the CAM2 runs with the idealized physical parameterization for the rotation periods of 0.5 day (a), 1 day (b), 5 days (c), 10 days (d), 16 days (e), 50 days (f), 150 days (g), and 243 days (h). Unit: K.

similar simulations of the Earth's atmosphere under different angular velocities/rotation periods. Besides, to see the different impact of dry and moist processes we adopted two physical parameterizations, an idealized physical parameterization and a complete physical parameterization. Fig. 6 shows the simulated vertical profiles of annual zonal-mean zonal wind from CAM2 runs for Earth's atmosphere. From the result of the idealized physical parameterization (upper panel in Fig. 6), a zonal wind collapse can be clearly seen in the relative slowing rotating regime (for the rotation periods between 5 and 50 days) and its intensity is stronger than that in the PGCM runs on Titan (Fig. 2). However, the height where the zonal wind collapse occurs varies with the rotation period. For the result of the complete physical parameterization (lower panel in Fig. 6) one only has a zonal wind collapse for some of the rotation periods, say 5 or 10 days; moreover, its intensity is weaker than that in the idealized physical parameterization. This implies that moist process may have an important impact on the zonal wind collapse.

Whether the idealized physical parameterization or the complete physical parameterization, superrotation phenomena of the simulated zonal winds occur in the slowly rotating regime (Fig. 7), same as the PGCM simulation on Titan. The result may confirm that superrotation is inevitable on slowly rotating planets with stable radiative equilibrium structures (Del Genio and Zhou, 1996). However, it is different from the previous study (Del Genio et al., 1993; Del Genio and Zhou, 1996) in that the strength of the superrotating zonal winds does not increase monotonously with rotation period in the slowly rotating regime. In the Earth's case, the strength of the simulated superrotating zonal winds increases with rotation period at the beginning and then decreases after a critical rotation period. This implies that the relationship between the strength of superrotation and rotation period is a complex non-linear relation rather than a linear relation. Besides, the strength of superrotating zonal winds is distinctly weaker in the complete physical parameterization than in the idealized physical parameterization, implying the significant influence of moist process.

The north–south horizontal temperature gradient is an important factor in the generation of zonal wind. We still employ the geotropic approximation for the zonal wind component and have the relation below

$$\frac{\partial u}{\partial p} = \frac{R}{pf}\frac{\partial T}{\partial y},$$

which implies that the zonal wind collapse may be related to large-scale meridional temperature gradient. Fig. 8 shows the vertical profiles of annual polar–equator temperature difference from the CAM2 runs with the idealized physical parameterization. It is obvious that the planetary-scale temperature difference is positive between 70 and 200 mbar for the rotation periods between 5 and 50 days, which are the rotating regime for the zonal wind collapse, implying that positive meridional temperatures are a necessary condition for the occurrence of zonal wind collapse.

5. Conclusions

We employed the PGCM to simulate the zonal wind collapse and atmospheric superrotation on Titan under different scenarios of angular velocities. The result implies that both the zonal wind collapse and the superrotation occur in the slowly rotating regime. However, the strength of the zonal wind collapse simulated by the PGCM is weaker than the observations, and furthermore, the simulated height of the zonal wind collapse on Titan is lower than the real one, which is something that needs to be reproduced by the PGCM through future improvements. The zonal wind collapse may also be associated with a large vertical slope of the buoyant stability. This is not apparent at high latitudes. Besides, the strength of the superrotating zonal winds on Titan increases with the rotation period in the slowly rotating regime, similar to the previous results (Del Genio and Zhou, 1996).

We also used the CAM2 to simulate the Earth's atmosphere under different cases of rotation speeds and compared the results with those of the Titan's atmosphere experiments from the PGCM, in order to identify the role of rotation period in the zonal wind collapse and the impact of other factors. The zonal wind collapse on Earth may happen mainly for a dry atmosphere in the case of rotation periods between 5 and 50 days. A positive meridional temperature gradient is a necessary condition for the zonal wind collapse. Moist processes may have a suppressive effect on the zonal wind collapse. Whether dry process or moist process, atmospheric superrotation exists in the slowing rotating regime but the amplitude of the superrotation is stronger in a dry atmosphere than in a moist atmosphere. Besides, the strength of superrotating zonal winds in Earth condition does not increase monotonously with rotation period in the slowly rotating regime, contrary to previous results.

To summarize, the results here show that a combination of a slowly rotating regime, dry processes, a large vertical slope of the buoyant stability, and a positive meridional temperature gradient is responsible for the zonal wind collapse. These findings require further theoretical verification and validation by comparison with the observational data.

Acknowledgments

We thank three anonymous referees, whose comments significantly improved the paper. This work was jointly supported by the 973 Program (2010CB950400) and the National Natural Science Foundation of China (41030961).

References

Barnes, J.R., Pollack, J.B., Haberle, R.M., Leovy, B., Zurek, R.W., Lee, H., Schaeffer, J., 1993. Mars atmospheric dynamics as simulated by the NASA Ames general circulation model. 2. Transient baroclinic eddies. Journal of Geophysical Research 98 (E2), 3125–3148.

Barnes, J.R., Haberle, R.M., Pollack, J.B., Lee, H., Schaeffer, J., 1996. Mars atmospheric dynamics as simulated by the NASA Ames general circulation model 3. Winter quasi-stationary. Journal of Geophysical Research 101, 12753–12776.

Bird, M.K., et al., 2002. The Huygens Doppler Wind Experiment. Space Science Reviews 104, 613–640.

Bird, M.K., Allison, M., Asmar, S.W., Atkinson, D.H., Avruch, I.M., Dutta-Roy, R., Dzierma, Y., Edenhofer, P., Folkner, W.M., Gurvits, L.I., Johnston, D.V., Plettemeier, D., Pogrebenko, S.V., Preston, R.A., Tyler, G.L., 2005. The vertical profile of winds on Titan. Nature 438, 800–802. doi:10.1038/nature04060.

Coustenis, A., Taylor, F.W., 2008. Titan: Exploring an Earth-like World. World Scientific Publishing, Singapore Eds.

Coustenis, A., et al., 2010. Titan trace gaseous composition from CIRS at the end of the Cassini-Huygens prime mission. Icarus 207, 461–476.

Collins, W.D., Hack, J.J., Boville, B.A., Rasch, P.J., Williamson, D.L., Kiehl, J.T., Briegled, B., Mccaa. J.R., Bitz, C., Lin, S.-J., Rood, R.B., Zhang, M.H., Dai Y.J., 2003. Description of the NCAR Community Atmosphere Model (CAM2). Boulder, Colorado 〈http://www.ccsm.ucar.edu/models/atm-cam/docs/cam2.0/description/index.html〉.

Del Genio, A.D., Zhou, W., Eichler, T.P., 1993. Equatorial superrotation in a slowly rotating GCM: Implications for Titan and Venus. Icarus 101, 1–17.

Del Genio, A.D., Zhou, W., 1996. Simulations of superrotation on slowly rotating planets: Sensitivity to rotation and initial condition. Icarus 120, 332–343.

Dowling, T.E., Bradley, M.E., Colón, E., Kramer, J., LeBeau, R.L., Lee, G.C.H., Mattox, T.I., Morales-Juberias, R., Palotai, C.J., Parimi, V.K., Showman, A.P., 2006. The EPIC atmospheric model with an isentropic/terrain-following hybrid vertical coordinate. Icarus 182, 259–273.

Dowling, T.E., Fischer, A.S., Gierasch, P.J., Harrington, J., LeBeau., R.P., Santori, C.M., 1998. The explicit planetary isentropic-coordinate (EPIC) atmospheric model. Icarus 132, 221–238.

Forget, F., Hourdin, F., Fournier, R., Hourdin, C., Talagrand, O., 1999. Improved general circulation models of the Martian atmosphere from the surface to above 80 km. Journal of Geophysical Research 104, 24155–24176.

Fulchignoni, M., 2007. Results on Titan's Atmosphere Structure by the Huygens Atmospheric Structure Instrument (HASI). The 4th AOGS, Bangkok, Thailand.

Grieger, B., Segschneider, J., Keller, H.U., Rodin, A.V., Lunkeit, F., Kirk, E., Fraedrich, K., 2004. Simulating Titan's tropospheric circulation with the Portable University Model of the Atmosphere. Advances in Space Research 34, 1650–1654.

Haberle, R.A., Murphy, J.R., Schaeffer, J., 2003. Orbital change experiments with a Mars general circulation model. Icarus 161, 66–89.

Haberle, R.M., Joshi, M.M., Murphy, J.R., Barnes, J.R., Schofield, J.T., Wilson, G., Lopez-Valverde, M., Hollingsworth, J.L., Bridger, A.F.C., Schaeffer, J., 1999. General circulation model simulations of the Mars Pathfinder atmospheric structure investigation/meteorology data. Journal of Geophysical Research 104 (E4), 8957–8974.

Haberle, R.M., Pollack, J.B., Barnes, J.R., Zurek, R.W., Leovy, C.B., Murphy, J.R., Lee, H., Schaeffer, J., 1993. Mars atmospheric dynamics as simulated by the NASA Ames general circulation model. 1. The zonal-mean circulation. Journal of Geophysical Research 98 (E2), 3093–3123.

Hartogh, P., Medvedev, A.S., Jarchow, C., 2007. Middle atmosphere polar warmings on Mars: Simulations and study on the validation with sub-millimeter observations. Planetary and Space Science 55, 1103–1112. doi:10.1016/j.pss.2006.11.018.

Hartogh, P., Medvedev, A.S., Kuroda, T., Saito, R., Villanueva, G., Feofilov, A.G., Kutepov, A.A., Berger, U., 2005. Description and climatology of a new general circulation model of the Martian atmosphere. Journal of Geophysical Research 110, E11008. doi:10.1029/2005JE002498.

Held, I.M., Suarez, M.J., 1994. A proposal for the intercomparison of the dynamical cores of atmospheric general circulation models. Bulletin of the American Meteorological Society 75, 1825–1830.

Hollingsworth, J.L., Barnes, J.R., 1996. Forced, stationary planetary waves in Mars' winter atmosphere. Journal of Atmospheric Science 53, 428–448.

Holton, J.R., 2004. An Introduction To Dynamic Meteorology. Elsevier Academic Press, Amsterdam [etc.] 534 pp.

Hourdin, F., Talagrand, O., Sadourny, R., Courtin, R., Gautier, D., McKay, C.P., 1995. Numerical simulation of the general circulation of the Titan. Icarus 117, 358–374.

Kuroda, T., Hashimoto, N., Sakai, D., Takahashi, M., 2005. Simulation of the Martian atmosphere using a CCSR/NIES AGCM. Journal of the Meteorological Society of Japan 83, 1–19.

Lebonnois, S., Hourdin, F., Rannou, P., Luz, D., Toublanc, D., 2003. Impact of the seasonal variations of composition on the temperature field of Titan's stratosphere. Icarus 163, 164–174.

Lebreton, J.-P. et al., 2005. An overview of the descent and landing of the Huygens probe. Nature 10.1038/nature04347.

Lee, C., Lewis, S.R., Read, P.L., 2005. A numerical model of the atmosphere of Venus. Advances in Space Research 36, 2142–2145.

Lee, C., Lewis, S.R., Read, P.L., 2007. Superrotation in a Venus general circulation model. Journal of Geophysical Research 112, E04S11. doi:10.1029/2006JE002874.

Lewis, S.R., Collins, M., Read, P.L., Forget, F., Hourdin, F., Fournier, R., Hourdin, C., Talagrand, O., Huot, J.O., 1999. A climate database for Mars. Journal of Geophysical Research 104 (E10), 24177–24194.

Li, J., Chou, J., 1998. Dynamical analysis on splitting of subtropical high-pressure zone—Geostrophic effect. Chinese Science Bulletin 43 (15), 1285–1289.

Liu, X.H., Li, J.P., Coustenis, A., 2008. A transposable planetary general circulation model (PGCM) and its preliminary application to Titan. Planetary and Space Science 56, 1618–1629.

Luz, D., Hourdin, F., Rannou, P., Lebonnois, S., 2003. Latitudinal transport by barotropic waves in Titan's stratosphere. II. Results from a coupled dynamics-microphysics-photochemistry GCM. Icarus 166, 343–358.

Moudden, Y., McConnell, J.C., 2005. A new model for multiscale modeling of the martian atmosphere, GM3. Journal of Geophysical Research 110, E04001. doi:10.1029/2004JE002354.

Murphy, J.R., Pollack, J.B., Haberle, R.M., Leovy, C.B., Toon, O.B., Schaeffer, J., 1995. Three-dimensional numerical simulation of Martian global dust storms. Journal of Geophysical Research 100 (E12), 26357–26376.

Pollack, J.B., Haberle, R.M., Murphy, J.R., Schaeffer, J., Lee, H., 1993. Simulations of the general circulation of the Martian atmosphere: 2. Seasonal pressure variations. Journal of Geophysical Research 98 (E2), 3149–3181.

Pollack, J.B., Haberle, R.M., Schaeffer, J., Lee, H., 1990. Simulations of the general circulation of the Martian atmosphere: 1. Polar processes. Journal of Geophysical Research 95 (B2), 1447–1473.

Pollack, J.B., Leovy, C.B., Greiman, P.W., Mintz, Y., 1981. A Martian general-circulation experiment with large topography. Journal of Atmospheric Sciences 38, 3–29.

Radebaugh, J., Lorenz, R.D., Kirk, R.L., Lunine, J.I., Stofan, E.R., Lopes, R.M.C., Wall, S.D., the Cassini Radar Team, 2007. Mountains on Titan observed by Cassini Radar. Icarus 192, 77–91.

Rannou, P., Hourdin, F., McKay, C.P., Luz, D., 2004. A coupled dynamics-microphysics model of Titan's atmosphere. Icarus 170, 443–462.

Richardson, M.I., Toigo, A.D., Newman, C.E., 2007. PlanetWRF: A general purpose, local to global numerical model for planetary atmospheric and climate dynamics. Journal of Geophysical Research 112, E09001. doi:10.1029/2006JE002825.

Rossow, W.B., 1983. A General Circulation Model of a Venus-Like Atmosphere. Journal of Atmospheric Sciences 40, 273–302.

Takahashi, Y.Q., Fujiwara, H., Fukunishi, H., Odaka, M., Hayashi, Y., Watanabe, S., 2003. Topographically induced north-south asymmetry of the meridional circulation in the Martian atmosphere. Journal of Geophysical Research 108 (E3), 5018. doi:10.1029/2001JE001638.

Takahashi, Y.Q., Odaka, M., Hayashi, Y.-Y., 2004. Martian Atmospheric General Circulation Simulation Simulated by GCM: A Comparison with the Observational Data. Bulletin of the American Astronomical Society 36, 1157.

Tokano, T., 2007. Dune-forming winds on Titan and the influence of topography. Planetary and Space Science 194, 243–262.

Tokano, T., Lorenz, R.D., 2006. GCM simulation of balloon trajectories on Titan. Planetary and Space Science 54, 685–694.

Tokano, T., Neubauer, F.M., Laube, M., McKay, C.P., 1999. Seasonal variation of Titan's atmospheric structure simulated by a general circulation model. Planetary and Space Science 47, 493–520.

Williamson, D.L., Olson, J.G., Boville, B.A., 1998. A comparison of semi- Lagrangian and Eulerian tropical climate simulations. Monthly Weather Review 126, 1001–1012.

Wilson, R.J., Hamilton, K., 1996. Comprehensive model simulation of thermal tides in the Martian atmosphere. Journal of Atmospheric Sciences 53, 1290–1326.

Wilson, R.J., Richardson, M.I., Clancy, R.T., Rodin, A.V., 1997. Simulation of Aerosol and Water Vapor Transport with the GFDL Mars General Circulation Model. Bulletin of the American Astronomical Society 29, 966.

Yamamoto, M., Takahashi, M., 2003. The fully developed super-rotation simulated by a general circulation model of Venus-like atmosphere. Journal of Atmospheric Sciences 60, 561–574.

Yamamoto, M., Takahashi, M., 2004. Superrotation Maintained by Meridional Circulation and Waves in a Venus-Like AGCM. Geophysical Research Letters 31, L09701. doi:10.1029/2004GL019518.

Young, R.E., Pollack, J.B., 1977. A three-dimensional model of dynamical processes in the Venus atmosphere. Journal of Atmospheric Science 34, 1315–1351.

Zhu, X., 2006. Maintenance of equatorial superrotation in the atmospheres of Venus and Titan. Planetary and Space Science 54, 761–773. doi:10.1016/j.pss.2006.05.004.